Available online at www.sciencedirect.com

ScienceDirect

Biomedical Journal

journal homepage: www.elsevier.com/locate/bj

Original Article

Spontaneous metastases in immunocompetent mice harboring a primary tumor driven by oncogene latent membrane protein 1 from Epstein–Barr virus

Pu-Yuan Chang [a,1], *Yenlin Huang* [b,1], *Tzu-Yuan Hung* [c], *Kowit-Yu Chong* [d], *Yu-Sun Chang* [c,e], *Chuck C.-K. Chao* [a,c,*], *Kai-Ping N. Chow* [c,f,**]

[a] *Tumor Biology Laboratory, Department of Biochemistry and Molecular Biology, College of Medicine, Chang Gung University, Taoyuan, Taiwan*

[b] *Department of Anatomic Pathology, Chang Gung Memorial Hospital at Linkou, Chang Gung University College of Medicine, Taoyuan, Taiwan*

[c] *Graduate Institute of Biomedical Sciences, College of Medicine, Chang Gung University, Taoyuan, Taiwan*

[d] *Department of Medical Biotechnology and Laboratory Science, College of Medicine, Chang Gung University, Taoyuan, Taiwan*

[e] *Molecular Medical Research Center, Chang Gung University, Taoyuan, Taiwan*

[f] *Department of Microbiology and Immunology, College of Medicine, Chang Gung University, Taoyuan, Taiwan*

ARTICLE INFO

Article history:
Received 24 May 2015
Accepted 9 December 2015
Available online 30 September 2016

Keywords:
Nasopharyngeal carcinoma (NPC)
Epstein–Barr virus (EBV)
Oncogene latent membrane protein 1 (N-LMP1)
Tumor mouse model
Distant metastasis

ABSTRACT

Background: In vitro and clinical studies suggest that the oncogene LMP1 (latent membrane protein 1) encoded by Epstein–Barr virus (EBV) plays a role in the development of nasopharyngeal carcinoma (NPC) and the formation of metastases in immunocompetent individuals. However, whether LMP1 itself is sufficient to drive these events in immunocompetent hosts remains elusive due to the lack of appropriate experimental models. The aim of this study was to study LMP1-dependent tumorigenesis and metastasis in BALB/c mice inoculated with BALB/c-3T3 cells expressing N-LMP1 (a Taiwanese NPC variant).

Methods: Following cancer cell inoculation, metastasis formation was monitored over time using PCR analysis of LMP1 as tumor marker. We also used a luciferase (Luc)-containing N-LMP1 and bioluminescent imaging (BLI) to monitor metastasis formation in a non-invasive manner.

Results: N-LMP1 appeared early in draining lymph nodes and in various distant organs before the rapid growth of the primary tumor. Lung metastasis was observed by BLI and

* *Corresponding author*. Tumor Biology Laboratory, Department of Biochemistry and Molecular Biology, College of Medicine, Chang Gung University, 259 Wenhua 1st Rd., Gueishan, Taoyuan 333, Taiwan. Tel.: +886 3 2118800ext.5151; fax: +886 3 2118700.

** *Corresponding author*. Department of Microbiology and Immunology, Graduate Institute of Biomedical Sciences, College of Medicine, Chang Gung University, 259 Wenhua 1st Rd., Gueishan, Taoyuan 333, Taiwan. Tel.: +886 3 2118800ext.5138; fax: +886 3 2118700.

E-mail addresses: cckchao@mail.cgu.edu.tw (C.C.-K. Chao), kpc@mail.cgu.edu.tw (K.-P.N. Chow).

Peer review under responsibility of Chang Gung University.

[1] Pu-Yuan Chang and Yenlin Huang contributed equally to this study.

http://dx.doi.org/10.1016/j.bj.2015.12.003

further confirmed by histological examination. Furthermore, we detected luciferase signals in the lungs, even before the animals were sacrificed.
Conclusions: Our results demonstrate the high metastatic character of N-LMP1 in immunocompetent hosts. Systemic tumor dissemination occurs even before aggressive tumor growth at the primary site, suggesting that early treatment of primary LMP1-associated tumors and distant micro-metastases is critical to achieve positive results.

At a glance commentary

Scientific background of the subject

Epstein–Barr virus (EBV)-encoded oncogene latent membrane protein 1 (LMP1) has been shown to play a role in the metastasis of nasopharyngeal carcinoma (NPC), an EBV-associated cancer that uniquely develops in immunocompetent individuals. We sought to examine whether and when LMP1 drives the formation of spontaneous metastasis in the immune intact host using a mouse tumor model established by N-LMP1, a LMP1 variant isolated from Taiwanese NPC patients.

What this study adds to the field

The primary tumor initiated by N-LMP1 showed high metastatic potential in the immunocompetent host. Systemic tumor dissemination occurred immediately after angiogenic switch but before aggressive tumor growth at the primary site. This finding suggests a critical time window for LMP1-based therapeutic interventions that could be used to concomitantly treat primary tumor and distant metastases.

Cancer is a leading cause of death worldwide and survival rates rapidly decline once metastases occur [1]. Metastasis development is a multi-step process characterized by the invasion-metastasis cascade [2–4]. This process involves cancer cell invasion into surrounding tissues, intravasation into nearby blood vessels, passage into the circulation, followed by homing into distant tissues, formation of new micrometastasis foci which eventually grow to form macroscopic secondary tumors. Tumor cell lines have been used to study the growth and motility of cancer cells following their inoculation into the tail vein of mice [5–7]. The role of the microenvironment is becoming more and more important in the study of factors regulating metastasis formation [8]. Unfortunately, *in vitro* cell culture does not reflect the importance of the microenvironment, nor does intravenous tail vein administration simulate the natural course of spontaneous metastasis. Therefore, establishing a spontaneous metastasis mouse model is of paramount importance in the study of tumor metastasis.

Bioluminescent imaging (BLI) has been recently developed to facilitate *in vivo* monitoring of cellular processes in various pathophysiological conditions [9–11]. BLI is a non-invasive imaging technique involving the generation of cold light by luciferase-expressing cells in animals following administration of luciferin substrate. Cold-light signals are then imaged using an external detector, allowing dynamic visualization of tumor-associated properties in living animals.

Nasopharyngeal carcinoma (NPC) is a malignant retronasal tumor that is endemic in Southern Asia and Taiwan [12]. Expression of the oncogene LMP1 (latent membrane protein 1) encoded by Epstein–Barr virus (EBV) has been associated with NPC pathogenesis [13]. NPC arises in immunocompetent hosts despite active humoral and cellular responses against EBV antigens at the systemic level [14]. Metastasis of NPC to regional lymph nodes and distant organs has been documented [15]. In clinical studies, LMP1 has been detected in local lymph nodes and distant tissues containing NPC metastasis by using immunohistochemistry. The cumulative metastasis rate has been estimated at 66.8% (269/403) in cases associated with LMP1 expression and 47.0% (148/315) in those where LMP1 expression is absent [16]. However, other studies have failed to demonstrate a link between LMP1 expression and the degree of tumor metastasis [17–19]. To date, metastasis development remains a problem in NPC treatment, and there are currently few animal models available to study spontaneous metastases in immunocompetent mice.

The cancer cell transformation role of LMP1 was initially described in a B-lymphoma, called B-LMP1 [20]. Later, LMP1 variants with a 30-nucleotide deletion at the 3′-end of the gene along with point mutations within the gene were observed in Chinese NPC [21,22]. The variant isolated from NPC patients in Taiwan, designated N-LMP1, shows the 30-nucleotide deletion but mutations at different regions than the ones identified previously [23]. In contrast to the prototype B-LMP1, N-LMP1-transfected BALB/c-3T3 cells (3T3/N-LMP1) exert a more potent oncogenic activity and form solid tumors in nude mice [24]. Studies have shown that N-LMP1 downregulates the expression of cell adhesion molecules; upregulates the activity of matrix metalloproteinases 1 and 9; and increases cell motility [25,26]. Furthermore, the invasive and metastatic potential of NPC cells is induced by N-LMP1 expression, and is inhibited when LMP1 expression is abrogated using small hairpin RNA *in vitro* and in immunodeficient mice [27,28]. However, whether tumor cells expressing N-LMP1 alone may metastasize in immunocompetent individuals has not been examined so far.

One characteristic of NPC is the massive leukocyte infiltration observed in tumor tissues [29], suggesting a role for components of the immune system in tumor pathogenesis. To study the contribution of immune cells in N-LMP1-driven oncogenesis, we previously established an N-LMP1-derived tumor model in syngeneic immunocompetent mice using tumorigenic 3T3/N-LMP1 cells [30]. Using this model, we report here the possibility to track tumor metastasis by using PCR analysis of N-LMP1 as tumor marker. Furthermore, we show that BLI can be used to follow the occurrence of spontaneous N-LMP1-derived tumor metastasis in immunocompetent hosts.

Methods

Mice

BALB/c and severe combined immunodeficiency (SCID) mice were purchased from the National Laboratory Animal Breeding and Research Center (Taipei, Taiwan) and BioLASCO (Ilan, Taiwan), respectively [30]. 6–10-week old mice were used in the experiments reported here. Animals were maintained in strict accordance with the NIH Guide for the Care and Use of Laboratory Animals, and animal experiment protocols were reviewed and approved by the Animal Ethics Committee of Chang Gung University.

Cell lines and N-LMP1 tumor model

The 3T3/N-LMP1 cell line (stable clone E2) established previously [23] was maintained at 37 °C in Dulbecco's modified Eagle's medium (DMEM) containing 10% fetal bovine serum (FBS). The N-LMP1 tumor model used in the present study was described earlier [30]. In brief, 3T3/N-LMP1 cells were injected into SCID mice to induce tumors. Tumor fragments of the initial tumor were transferred into BALB/c mice by subcutaneous transplantation. Subsequently, tumor lines were passaged *in vivo* in BALB/c mice every 3–4 weeks. The day of transplantation was designated as day 0. Tumor volume was determined using the following formula: volume = width × length × height × 0.52. The same strategy was used to establish the bioluminescent E2-Luc model using E2-Luc tumor cell line (see below).

Polymerase chain reaction (PCR)

Genomic DNA was extracted from different animal organ and tissues. The primers, PCR reaction conditions and gel electrophoresis for N-LMP1 and internal control GAPDH were described previously [30,31]. N-LMP1 primers: sense primer (5′-GGTTGATCTCCTTTGGCTCCTCCTG-3′) and antisense primer (5′-GTCAGTCAGGCAAGCCTATGACATG-3′). GAPDH primers: sense primer (5′-TGGTATCGTGGAAGGACTCATGAC-3′) and antisense primer (5′-ATGCCAGTGAGCTTCCCGTTCAGC-3′). Luciferase primers: sense primer (5′-TCAAAGAGGCGAACTGTGTG-3′) and antisense primer (5′-GGTGTTGGAGCAAGATGGAT-3′).

Establishment of E2-Luc stable cell line

A 2.5-kb fragment containing the complete coding region of luciferase-EGFP was released from the pL3-TRE-LucGFP-2L plasmid (Addgene, Cambridge, MA, USA) by SacII and EcoRV double digestion. The DNA fragment was then ligated into a lentiviral vector, pLenti 6.2 (Life Technologies), designated pLenti-LucEGFP [32]. A lentivirus carrying LucEGFP was used to transduce E2 cells. GFP/Luc-infected E2 cells (E2-Luc) were trypsinized and washed with phosphate-buffered saline (PBS) and put on ice. To collect GFP-positive cells, the isolated E2-Luc cells (1×10^6) were resuspended in 500 μl PBS and GFP-positive cells were sorted using a FACScan flow cytometer (Becton Dickinson, CA, USA). Fluorescence emission for GFP was determined at 530 nm (FLI). Acquisition was performed automatically using the CellQuest Pro software (Becton Dickinson).

To enrich Luc image, virus-infected E2 cells (carrying the EGFP-Luc plasmid) were grown for 14 days *in vitro* and subjected to two rounds of cell sorting against EGFP. The first sorted cells were grown for 12 days *in vitro* before the second sorting. The LMP1-positive cells enriched by cell sorting were used for animal experiments.

MTT assay

Cell viability was determined using the 3-(4,5-dimethylthiahiazo-2-yl)-2,5-di-phenytetrazoliumromide (MTT) colorimetric assay. Briefly, E2 or E2-Luc cells (10^3) were cultured in 96-well plates. The culture medium (100 μl) was changed on day 3 and 5. MTT solution (0.5 mg in PBS) was added into the wells and incubated for 4 h. Supernatants were collected and formazan was dissolved with 150 μl of DMSO, following reading at a wavelength of 570 nm.

Anchorage-independent colony forming assay

The anchorage-independent growth of E2 and E2-Luc cells was assessed by soft-agar colony formation assay. Cells (1.5×10^3) were resuspended in 3 ml of DMEM containing 10% FBS and 0.7% agar and added over a layer of 5 ml of the same medium containing 1% agar in 6-well culture plates. Three-weeks later, colonies were stained with a solution of 0.04% crystal violet and 2% ethanol in PBS. Photographs of the stained colonies were taken and colony numbers were counted.

Transwell assay

Transwell plates with a membrane filter (6.5 mm diameter, 8 μm pore size; BD Biocoat, New Jersey, NJ, USA) were used to measure cell migration. The upper chamber contained either E2 or E2-Luc cells in serum-free medium (8×10^4/100 μl), and the lower chamber contained 600 μl of FBS-containing medium. Twenty hours later, cells left on the upper surface of the membrane were scraped with a cotton swab. Cells on the bottom membrane surface were stained with a crystal violet solution and counted under the microscope.

In vitro *bioluminescence assay*

E2-Luc cells were permeabilized by luciferase cell lysis buffer (Promega, WI, USA) and the protein extract was quantified using the SpectraMax 340PC384 ELISA reader (Molecular devices, CA, USA). Bioluminescent intensity was then measured by mixing 25 μg of protein with 100 μl luciferin (Beta-Glo Assay System, Promega) using Dual-Luciferase Assay System (Promega).

In vivo *bioluminescence assay*

Mice bearing subcutaneous E2-Luc tumors were injected intraperitoneally with the luciferase substrate D-luciferin (125 mg/kg, Sigma). Mice were placed in a dark chamber of the IVIS 100 imaging system (Xenogen, Alameda, CA, USA) under isoflurane anesthesia. Photographic and bioluminescent images (BLI) were captured according to the manufacturer's instructions.

Tumor histology

Tumor specimens and mice organs were fixed in 10% formalin, embedded in paraffin and sectioned for light microscopy. Tumor sections (5 μm) were stained with hematoxylin and eosin (H&E) as described [30].

Statistical analysis

Data analysis was performed using the Microsoft Excel software. Student t-test was used in the experiments. The values presented are expressed as mean ± standard deviation (SD). A level of 0.05 was considered to be statistically significant.

Results

Dissemination potential of N-LMP1-expressing cancer cells

N-LMP1 is the prevalent LMP1 variant in Taiwanese NPC patients [21,23]. Previous studies have demonstrated that 3T3/N-LMP1 cells (e.g., clone E2) can form tumors in syngeneic immunocompetent mice following subcutaneous transplantation of tumor fragments derived from nude (or SCID) mice. In this model, tumor development occurs during the first two weeks, but exponential growth occurs during week 2–3 [30]. By using non-invasive dynamic contrast-enhanced magnetic resonance imaging, we have identified an angiogenic switch period between days 7–14 prior to rapid tumor expansion [33]. To further characterize whether and when N-LMP1 tumors disseminate, we examined the presence of LMP1 DNA in various tissues on day 5–28 using PCR analysis. To ensure the detection of tumor cells homed to (instead of temporarily passing by) the tissues [34,35], tumor-bearing mice were perfused with PBS before removing organs for DNA extraction. N-LMP1 DNA was detected in draining lymph nodes as early as day 7 [Fig. 1]. N-LMP1 DNA was also detected in the thymus and spleen in some mice at day 15–17. N-LMP1 DNA signal was also detected in the liver and lungs. After day 15–17, the signal remained high in the lymph nodes, liver, lungs and thymus. These results indicate that dissemination of N-LMP1 tumor cells to draining lymph nodes occurs early (within 7 days) following tumor formation.

A

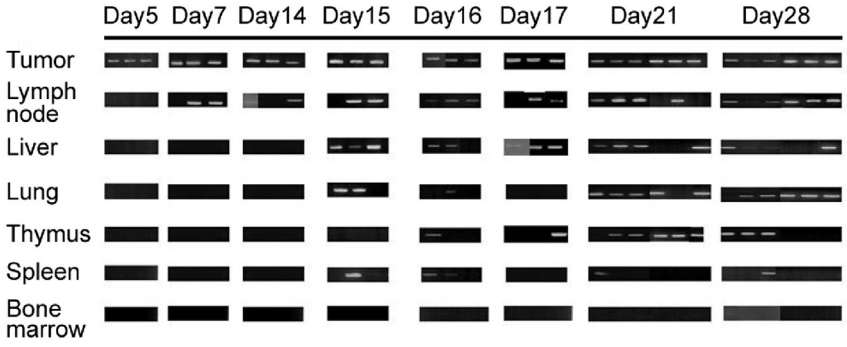

B

N-LMP1 PCR	Day5 N=3	Day7 N=3	Day14 N=3	Day15 N=3	Day16 N=3	Day17 N=3	Day21 N=6	Day28 N=6
Tumor	●●●	●●●	●●●	●●●	●●●	●●●	●●●●●●	●●●●●●
Lymph node	○○○	●●○	●●○	●●○	●●●	●●○	●●●●○○	●●●●●●
Liver	○○○	○○○	○○○	●●●	●●○	●●●	●●●●○○	●●●●○○
Lung	○○○	○○○	○○○	●●○	●○○	○○○	●●●●●○	●●●●●○
Thymus	○○○	○○○	○○○	○○○	●○○	●○○	●●●●●○	●●●○○○
Spleen	○○○	○○○	○○○	●●○	●●○	○○○	●○○○○○	●○○○○○
Bone marrow	○○○	○○○	○○○	○○○	○○○	○○○	○○○○○○	●○○○○○

Fig. 1 – Potential of E2 tumor metastasis. (A) The presence of N-LMP1 DNA was identified by PCR assay in the indicated organs from E2 tumor-bearing SCID mice at the indicated time points (N = 3 or 6). (B) Organs with positive (black circles) or negative (white circle) PCR signals from (A) are shown.

Establishment of the E2-Luc cell line

We next sought to establish a Luc-bearing E2 tumor model, in an attempt to visualize in a non-invasive manner the development of micro- and macro-metastases after cancer cell dissemination. We used an animal model based on a Luc-positive 3T3/N-LMP1 cell line as described earlier [30]. Accordingly, E2-Luc cells were enriched by flow cytometry [Fig. 2A, see Method for details]. The GFP-positive cell fraction only represented 66.55% of the cell population before sorting but reached 91.75% and 95.27% after the first and second sorting steps, respectively. The E2-Luc cell line exerted stable luciferase activity, giving a luciferase intensity between 60–120 × 10^6 over 25 passages (Fig. 2B). To understand

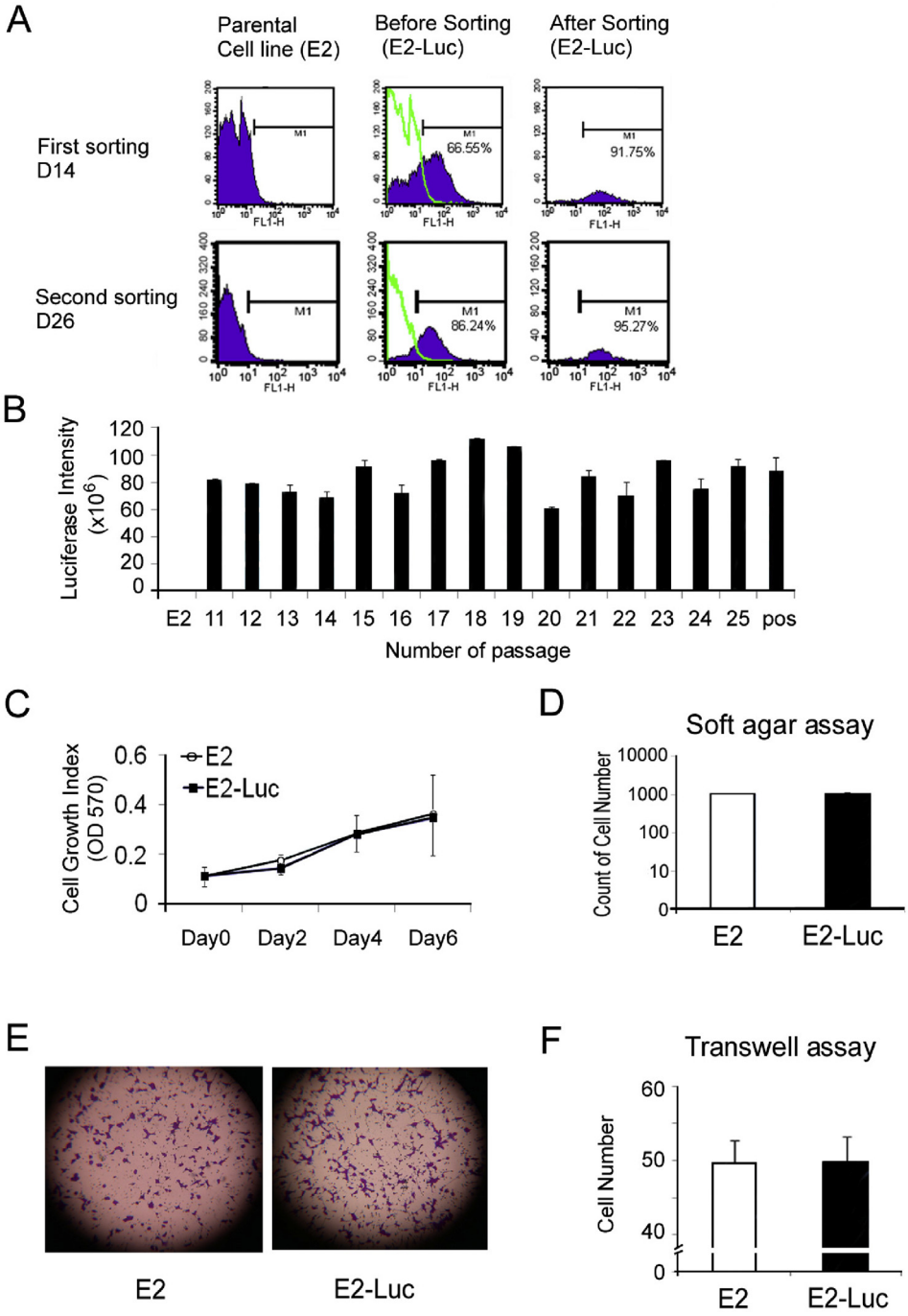

Fig. 2 – Establishment of E2-Luc cell line. (A) GFP/Luc-tranduced E2 cells underwent two (D14 and D26) cell sortings based on the collection of GFP positive cells by flow cytometry. (B) E2-Luc cell line showed stable luciferase activity over 25 passages. Cell growth was estimated using the MTT assay (C) and soft agar assay (D). Cell migration was analyzed using the transwell assay (E) and quantitative analysis is shown in (F). E2-Luc cells were not statistically different than parent E2 cells in terms of both cell growth and cell migration results. Data represent means ± SD.

whether the luciferase/eGFP plasmid affected the cells, we compared the growth of E2 and E2-Luc cells using the MTT assay (Fig. 2C). In addition, the tumorigenic and invasive potentials of the cells were examined using respectively the soft agar assay (Fig. 2D) and transwell migration assay (Fig. 2E,F). The tumorigenic and invasive potentials of E2-Luc cells and parental E2 cells were similar, indicating that luciferase/eGFP transfection did not alter cellular functions.

Luciferase activity of E2-Luc tumors in SCID mice

In vivo tumorigenicity of E2-Luc cells was examined by injecting the cells subcutaneously into SCID mice. The formation of Luc-positive tumors was monitored between week 1–4 using the BLI system [Fig. 3A]. Tumor growth was quantified by measuring luciferase intensity as a function of time (Fig. 3B). E2-Luc cells demonstrated strong tumorigenicity as seen by the formation of palpable tumors two weeks after induction, with continuous growth occurring between week 2–4.

Partial loss of luciferase activity of E2-Luc tumors in BALB/c mice

To induce E2-Luc tumor formation in BALB/c mice, tumor fragments derived from tumor-bearing SCID mice (mouse #3 in Fig. 3) were transplanted into BALB/c mice [Fig. 4A]. As persistent expression of luciferase activity in the tumor mass is a critical feature for a usable animal model, we examined the duration of the luciferase signal in transplanted tumors *in vivo*. Surprisingly, while the luciferase signal of E2-Luc tumors was detected at day 7 following transplantation in BALB/c mice, the signal was entirely lost at day 42 (Fig. 4A and B). No luciferase activity was detected in the region of E2-Luc tumors in which light signal was lost (Fig. 4C, dark region), although luciferase DNA was still detected by PCR in both the bright and dark tumor regions (Fig. 4D). These results suggest that luciferase expression was dramatically suppressed in transplanted E2-Luc tumors. Besides, we observed that tumor growth was similar in BALB/c and SCID mice (data not shown). Together, these results suggest partial loss of luciferase activity of E2-Luc tumors in BALB/c mice.

Establishment of a stable E2-Luc tumor line by successive in vivo passages from the luminescence-positive tumor fragments of BALB/c mice

To access whether the E2-Luc cancer cell line can consistently express luciferase, we transplanted fragments of luciferase-positive bright tumor tissues from BALB/c mice (mouse #3 in Fig. 4, was assigned as passage 0, labeled as P0) into 5 naive BALB/c mice, followed by a series of *in vivo* passages from P0 to P4. BLI observation was performed at the days indicated [Fig. 5A]. Luciferase intensity of different passages (P1–4) tumors from was also quantified (Fig. 5B). Tumor growth of different passages, including of E2 parental tumors and E2-Luc tumors P0–4, was measured (Fig. 5C). BLI images showed that early passages (P0, P1, P2) still contained the tissues that had lost luciferase activity, and the tumor growth was slower than parental E2 tumors. Luminescent areas and tumor growth increased in later passages (P3, P4), approaching the levels observed for parental E2 tumors.

Identification of lung metastasis derived from E2-Luc tumors in BALB/c mice

To assess systemic metastasis dissemination, mice of passages 0–7 (P0–P7) were sacrificed at day 28. Local tumors and

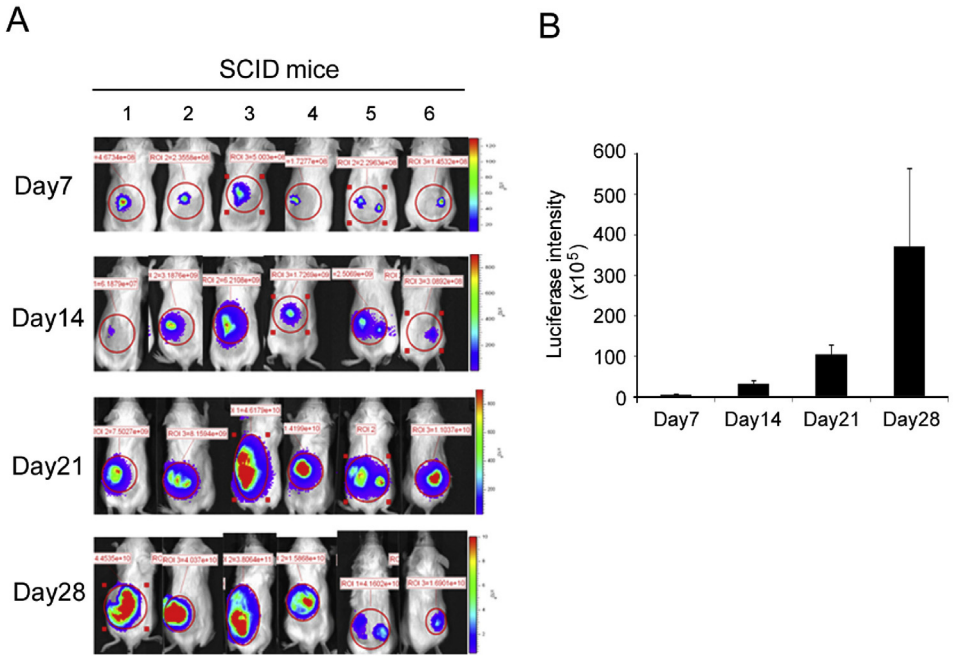

Fig. 3 – Tumor growth and BLI signal quantification of E2-Luc tumor in SCID mice. (A) E2-Luc cells were subcutaneously injected in the back of mice (numbered 1–6) at day 1. BLI was performed on day 7, 14, 21, and 28. (B) Luciferase intensity of 6 mouse tumors was quantified at the indicated days. Data represent means ± SD.

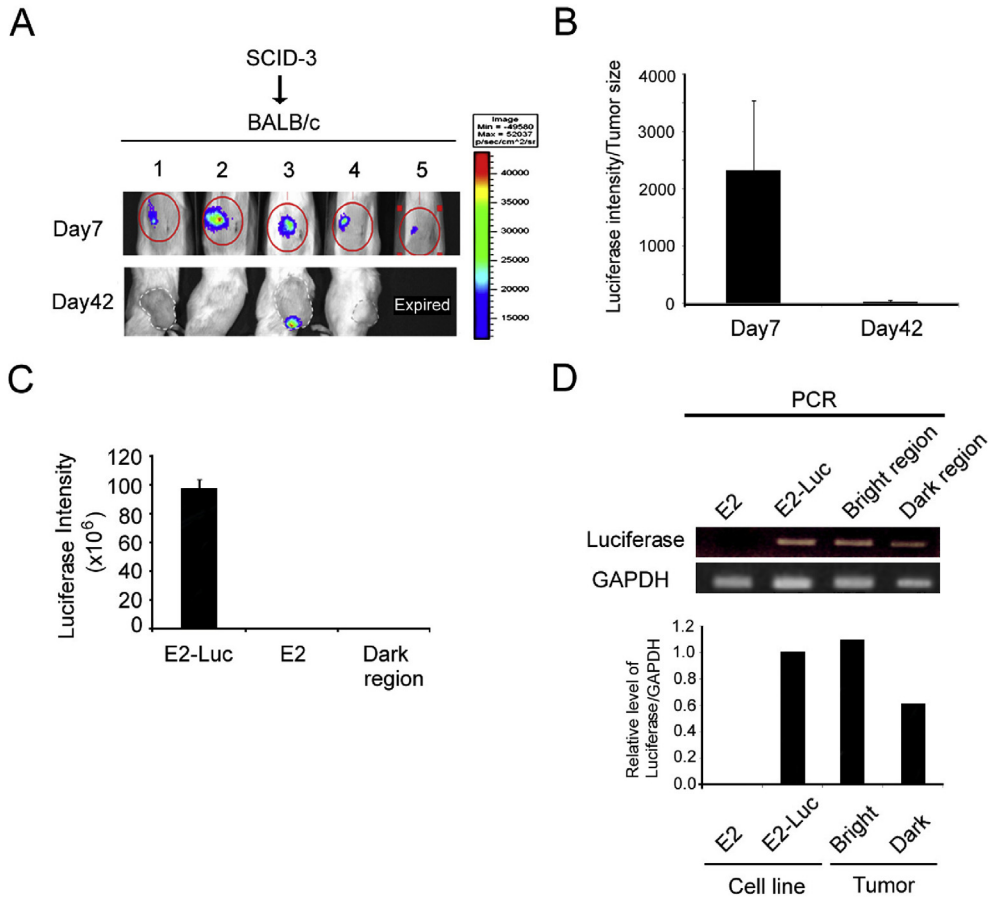

Fig. 4 – Tumor growth and BLI signal loss in E2-Luc tumors in BALB/c immunocompetent mice. Fragments of E2-Luc tumors from SCID mice (#3 mouse in Fig. 3) were transplanted into BALB/c mice (numbered 1–5). (A, B) BLI was performed at day 7 and day 42 and luminescence signals were detected and quantified. Data are presented as mean ± SD. (C) There was no luciferase activity in the loss light signal region (dark region) of E2-Luc tumors in BALB/c mice. The E2-Luc cell line showed luciferase activity as positive control and E2 cell as negative control. (D) The presence of luciferase DNA in the bright or dark tumor regions was identified by PCR assay. The E2 cell line was used as negative control and E2-Luc as positive control. GAPDH was used as internal control.

various organs (lung, spleen, liver, lymph nodes and thymus) were removed to perform *ex vivo* BLI [Fig. 6A,B], followed by histological examination. Luciferase activity was detected in local tumors, predominantly in the lungs and some lymph nodes, implying that E2-Luc tumors could progress to form metastases which could be detected *ex vivo* at the whole tissue level. By using H&E staining, we observed that the majority of lung tissue sections harbored metastatic tumor nodules, as exemplified here by a P7 mouse (Fig. 6C). Concordance between BLI signals the presence of N-LMP1 DNA was further verified by PCR analysis (Fig. 6D). N-LMP1 DNA could be detected in the corresponding tissues of the tested mice, mainly in the lungs. Although N-LMP1 DNA and/or BLI was detected in some other organs such as lymph nodes and liver, no pathological tumor nodules could be found (data not shown), suggesting that the lung is the preferential target organ for N-LMP1 tumor metastasis in this animal model. As metastasis usually involves a low number of cells colonized in internal organs, prolonged exposure may be required. In this animal model, we found that the internal metastatic organs require an exposure time of at least 30 s. Since local primary tumors show much more luminescence intensity, distant organ metastasis with relatively low luminescence signal will be overwhelmed by a strong local tumor luminescence signal, making it impossible to explore tumor metastasis. To overcome this problem, we shielded the strong luminescence signal of tumors by using black card. *In vivo* BLI image luciferase activity from lung-like regions could be detected directly (red circle, Fig. 6E, left panel). Together with the *ex vivo* BLI images of the lungs, liver, spleen, thymus, and lymph nodes observed after *in vivo* BLI, only the lungs could be shown to produce a positive signal (Fig. 6E, right panel).

Discussion

The metastasis-inducing character of LMP1 has been suggested in various *in vitro* and clinical studies [15,25]. However, whether the expression of LMP1 alone in cancerous cells could lead to the formation of distant metastases in

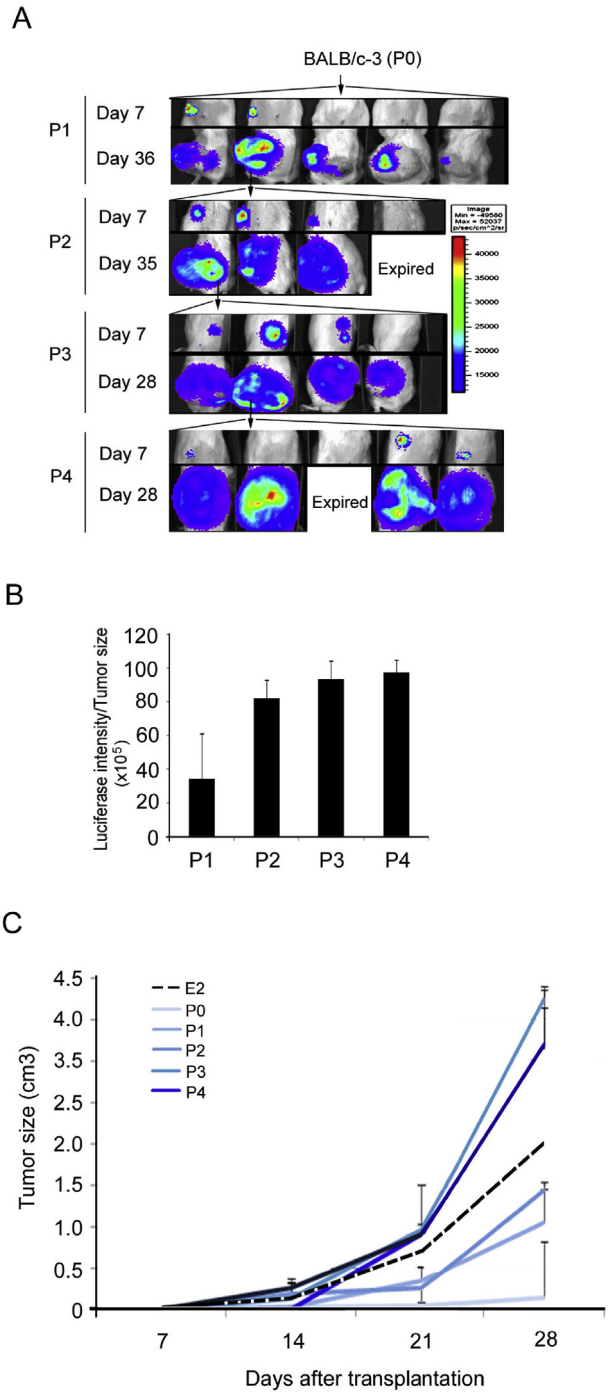

Fig. 5 – A stable *in vivo* E2-Luc tumor line was established by series of *in vivo* passages from the luciferase-positive bright tumor tissue of BALB/c mice (#3 mouse in Fig. 4, was assigned as passage 0, P0). Luminescence-positive tumor tissues were transplanted from passage 1–4 (P1–4). BLI images were obtained (A) at the indicated days. Arrows indicated the mouse was selected for tumor transplantation. (B) Luciferase intensity of different passages (P1–4) tumors from (A) was quantified. (C) The tumor growth curve of different generations (E2 parent tumor, E2-Luc tumor P0–5) was shown on. Data represent means ± SD.

immunocompetent host has remained obscure. In the present study, a tumor model system that we established previously [30] was simplified to highlight the interaction between N-LMP1 and the immune system during tumor progression. By using this system, our results demonstrate early systemic dissemination and natural lung metastasis formation from primary N-LMP1 tumors, suggesting that N-LMP1 may be involved in both tumor initiation and metastasis formation in spite of an intact host immune system.

Our data suggest that N-LMP1 tumor cells could spread to the draining lymph nodes at an early time. This finding is consistent with previous clinical studies that observed proximal metastasis of regional lymph nodes in the early stage of NPC development [36,37]. Moreover, our results also indicate that the dissemination to distant organs occurs before the rapid growth of primary tumors, supporting the emerging notion that tumor cell dissemination may take place early and that it may not necessarily be a late event during cancer progression [4,38–40]. While primary tumors undergo angiogenic switch at days 7–14 [33], the appearance of LMP1 in distant organs at days 15–17 implies that dissemination can occur as soon as tumor neovasculature is established. Although bone metastasis of NPC in clinical cases is frequent [36], LMP1 in bone marrow was not detected in our model system (see Fig. 1B). As the microenvironment at the primary tumor site is believed to play an important role for the formation of distant metastases [7,41], the lack of bone dissemination may suggest that N-LMP1 alone is insufficient to influence this specific site. Other viral and host factors may be essential for bone marrow dissemination [41–43]. Alternatively, because the experimental cell line used in this study is a 3T3/N-LMP1 cell line which is different from the epithelial nature of NPC, the microenvironment might not be important for 3T3 cell lodging into the bone marrow.

In this study, a bioluminescent N-LMP1 tumor model was established for the assessment of spontaneous metastasis formation. As suggested by *in vitro* and *in vivo* analyses, the high carcinogenicity of E2 cells was stably maintained in E2-Luc cells and the luminescence intensity showed positive correlation with tumor growth in SCID mice. However, when tumors were transplanted into BALB/c mice, BLI signal declined with time. Several factors may explain the disappearance of luminescence intensity. One possibility is that the luciferase gene still existed, but was suppressed by host factors (such as cytokines), which can inhibit the CMV promoter that drives luciferase expression [44]. PCR detection of the dark tumor area which showed no luminescence activity indicated that luciferase gene indeed still existed (Fig. 4D), implying that its expression may have been down-regulated by the immunocompetent host. Furthermore, since both GFP and luciferase are foreign protein antigens which possibly bear immunogenicity, it is possible that E2-Luc cells down-regulated luciferase expression to avoid host immune defense. Nonetheless, we established a stable E2-Luc tumor line of BALB/c mice by a series of *in vivo* passages from the luciferase-positive tumor graft.

BLI observations in BALB/c host suggested a high probability of metastasis in the lungs and lymph nodes (Fig. 5B),

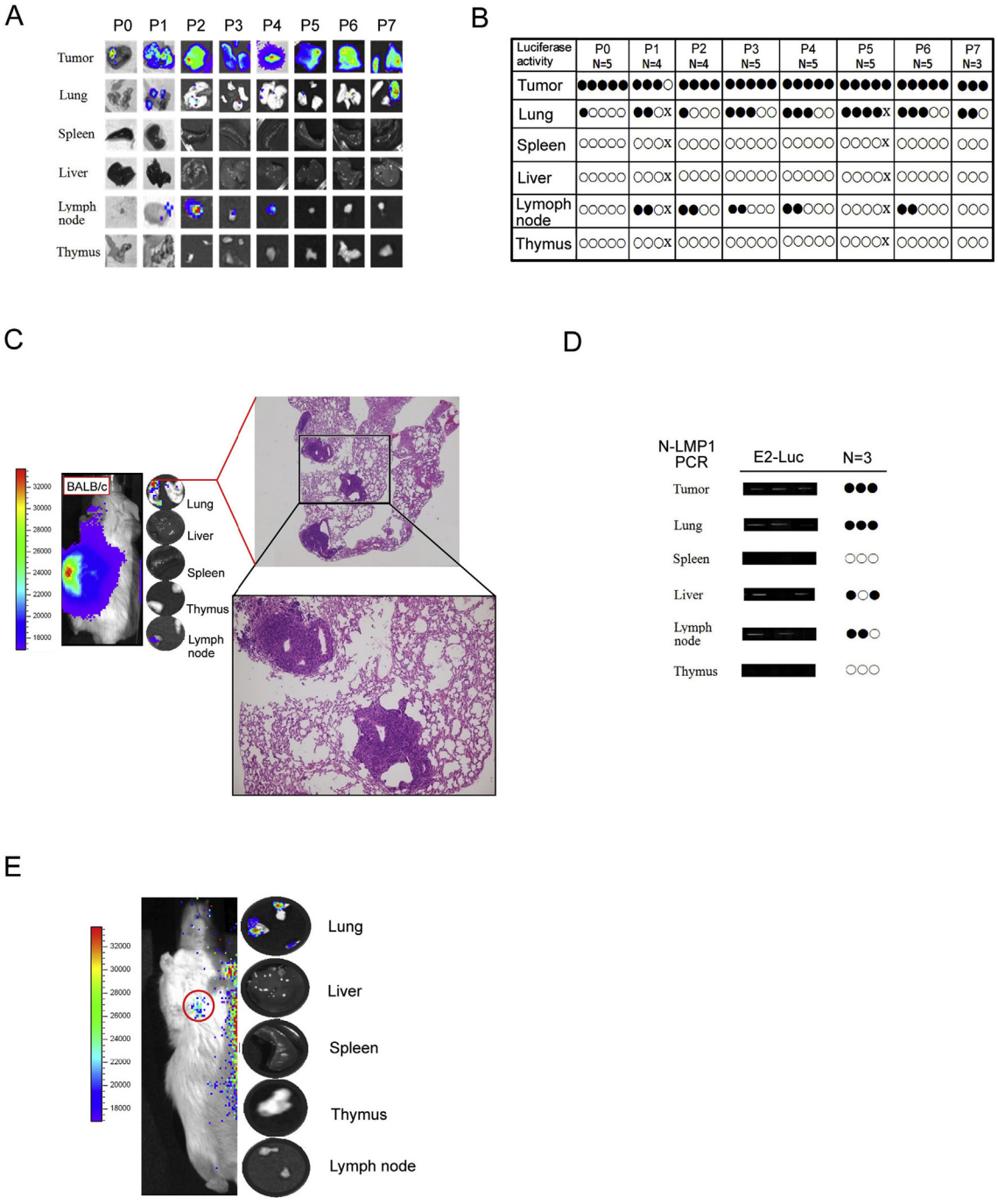

Fig. 6 – Metastasis of E2-Luc tumor in BALB/c mice. Mice of passages 0–7 (P0–P7) were sacrificed at day 28. Local tumor and various organs were removed to perform BLI *ex vivo* (A, B) followed by histological examination (C). (A) Representative *ex vivo* BLI images of lungs, spleen, liver, lymph nodes, and thymus. Lung and lymph nodes were shown with positive signals. (B) Organs with (black circles) or without (white circles) luminescence from (A) are shown. (C) Representative H&E-stained tissue sections of positive BLI region showed only lung tissues with tumor nodules. (D) The presence of LMP1 DNA in the indicated organs of E2-Luc tumor-bearing mice was detected by PCR assay at day 21 in an independent experiment. Organs with positive (black circles) or negative (white circles) PCR signals are indicated. (E) Representative *in vivo* BLI images revealed metastatic E2-Luc cell luciferase activity in lung tissues. The strong luminescence signal of the local primary tumor was shielded by black card (the red circle on the mouse indicated that BLI signal originated from lung-like regions).

indicating that after systemic dissemination only few distant sites could proceed into metastasis. H&E stained tissues showed that lung tumors were indeed present, suggesting possible E2-Luc cell colonization, but with no signs of tumor metastases to other organs. It is possible that early dissemination of tumor cells to the lymph nodes (day 7) may remain dormant at low cell numbers, being unable to successfully colonize the immunocompetent microenvironment.

The *in vivo* BLI system is based on the relationship between the detection sensitivity and cell numbers. Our ultimate goal was to visualize tumor progression (local and metastasis) non-invasively by keeping animals alive for longitudinal imaging. As metastasis usually involves low number of cells colonized in the internal organs, prolonged exposure time is required to obtain tumor image. In this model, we found that the internal metastatic organs require an exposure time to at least 30 s. In this situation, the local primary tumor is much more luminescent than the metastases. Distant organ metastasis with relatively low luminescence signal will be overwhelmed by a strong local tumor luminescence signal, making it impossible to explore tumor metastasis. Nevertheless, by using a shield of black cardboard and BLI observation from the side of animals, luminescence from the lung region could be detected. Although some of our objectives could not be achieved due to technical limitations, the luminescent N-LMP1 tumor model could still serve as a powerful screening tool for *ex vivo* tracking of tumor metastases in future studies.

In this study, no metastatic tumors were observed in the bone marrow. Since the experimental cell line used in this study is 3T3/N-LMP1 which is different from the epithelial nature of NPC, it is possible that the microenvironment is not important for 3T3 cell lodging in the bone marrow. We noted that a NIH3T3 fibroblast-derived cancer cell produced by LMP1 expression may not be truthfully representative of LMP1-transformed epithelial cancer as LMP1-associated NPC. Although this model can not be used to fully explain oncogenesis and metastasis of epithelial tumors like NPC, our results still demonstrated the high metastatic character of N-LMP1 in immunocompetent host. Our results also showed that systemic cancer cell dissemination could occur before the aggressive tumor growth of at the primary site. In addition, due to the fact that tumor cells are implanted directly into the organ of origin, these tumors reflect the original situation (e.g., the microenvironment) much better than conventional subcutaneous tumor models. It will be more realistic if these results can be verified by taking orthotopic tumor models rather than standard subcutaneous models. Nevertheless, the results of this study may reveal critical insights applicable to clinical settings.

Taken together, our results demonstrate the high potential of early systemic dissemination and metastasis of N-LMP1-expressing primary tumors. The study of spontaneous metastasis may better reflect the development of metastasis occurring *in vivo*; our system can therefore be used as a platform for the study of future cancer therapeutics targeting LMP1 in NPC. In particular, our study shows the precise timing of multi-organ spreading with tumor angiogenic transition [45], suggesting a critical time window to treat primary tumors and distant metastases.

Conflicts of interest

The authors have no financial conflicts of interest.

Acknowledgements

Pu-Yuan Chang: Design, Literature search, Experimental studies, Data analysis, Manuscript preparation, Manuscript editing. Yenlin Huang: Definition of intellectual content, Literature search, Clinical studies, Data analysis, Manuscript preparation. Tzu Yuan Hung: Design, Literature search, Experimental studies, Data analysis. Kowit-Yu Chong: Concepts, Design. Yu-Sun Chang: Concepts, Definition of intellectual content, Manuscript review. Chuck C.-K. Chao: Concepts, Design, Definition of intellectual content, Manuscript preparation, Manuscript editing and review. Kai-Ping N. Chow: Concepts, Design, Definition of intellectual content, Literature search, Experimental studies, Data analysis, Manuscript preparation, Manuscript editing and review.

We are grateful to H-B Li for technical assistance, and the Center for Advanced Molecular Imaging and Translation, Chang Gung Medical Foundation for imaging data analysis. This work was supported by grants from Chang-Gung Memorial Hospital (grants CMRPD1C0063, CMRPG3C0962, CMRPG3A1233 and NMRPG3C6142) and Taiwan Ministry of Science and Technology (grant NSC102-2320-B-182A-006-MY3).

REFERENCES

[1] Teo PM, Kwan WH, Lee WY, Leung SF, Johnson PJ. Prognosticators determining survival subsequent to distant metastasis from nasopharyngeal carcinoma. Cancer 1996;77:2423–31.
[2] Klein CA. Cancer. The metastasis cascade. Science 2008;321:1785–7.
[3] Nguyen DX, Bos PD, Massague J. Metastasis: from dissemination to organ-specific colonization. Nat Rev Cancer 2009;9:274–84.
[4] Valastyan S, Weinberg RA. Tumor metastasis: molecular insights and evolving paradigms. Cell 2011;147:275–92.
[5] Murakami T, Cardones AR, Hwang ST. Chemokine receptors and melanoma metastasis. J Dermatol Sci 2004;36:71–8.
[6] Joyce JA, Pollard JW. Microenvironmental regulation of metastasis. Nat Rev Cancer 2009;9:239–52.
[7] Quail DF, Joyce JA. Microenvironmental regulation of tumor progression and metastasis. Nat Med 2013;19:1423–37.
[8] Tse JC, Kalluri R. Mechanisms of metastasis: epithelial-to-mesenchymal transition and contribution of tumor microenvironment. J Cell Biochem 2007;101:816–29.
[9] Villablanca EJ, Raccosta L, Zhou D, Fontana R, Maggioni D, Negro A, et al. Tumor-mediated liver X receptor-alpha activation inhibits CC chemokine receptor-7 expression on dendritic cells and dampens antitumor responses. Nat Med 2010;16:98–105.
[10] Grosse-Wilde A, Voloshanenko O, Bailey SL, Longton GM, Schaefer U, Csernok AI, et al. TRAIL-R deficiency in mice enhances lymph node metastasis without affecting primary tumor development. J Clin Invest 2008;118:100–10.
[11] Yanagisawa S, Kadouchi I, Yokomori K, Hirose M, Hakozaki M, Hojo H, et al. Identification and metastatic potential of tumor-initiating cells in malignant rhabdoid tumor of the kidney. Clin Cancer Res 2009;15:3014–22.

[12] Chang ET, Adami HO. The enigmatic epidemiology of nasopharyngeal carcinoma. Cancer Epidemiol Biomarkers Prev 2006;15:1765–77.
[13] Baichwal VR, Sugden B. Transformation of Balb 3T3 cells by the BNLF-1 gene of Epstein–Barr virus. Oncogene 1988;2:461–7.
[14] Jung S, Chung YK, Chang SH, Kim J, Kim HR, Jang HS, et al. DNA-mediated immunization of glycoprotein 350 of Epstein–Barr virus induces the effective humoral and cellular immune responses against the antigen. Mol Cell 2001;12:41–9.
[15] Leung SF, Teo PM, Shiu WW, Tsao SY, Leung TW. Clinical features and management of distant metastases of nasopharyngeal carcinoma. J Otolaryngol 1991;20:27–9.
[16] Zhao Y, Wang Y, Zeng S, Hu X. LMP1 expression is positively associated with metastasis of nasopharyngeal carcinoma: evidence from a meta-analysis. J Clin Pathol 2012;65:41–5.
[17] Li J, Zhang XS, Xie D, Deng HX, Gao YF, Chen QY, et al. Expression of immune-related molecules in primary EBV-positive Chinese nasopharyngeal carcinoma: associated with latent membrane protein 1 (LMP1) expression. Cancer Biol Ther 2007;6:1997–2004.
[18] Liu Q, Han A, You S, Yang Q, Liang Y, Dong Y. The association of genomic variation of Epstein–Barr virus BamHI F fragment with the proliferation of nasopharyngeal carcinoma. APMIS 2010;118:657–64.
[19] Jeon YK, Lee BY, Kim JE, Lee SS, Kim CW. Molecular characterization of Epstein–Barr virus and oncoprotein expression in nasopharyngeal carcinoma in Korea. Head Neck 2004;26:573–83.
[20] Kaye KM, Izumi KM, Kieff E. Epstein–Barr virus latent membrane protein 1 is essential for B-lymphocyte growth transformation. Proc Natl Acad Sci USA 1993;90:9150–4.
[21] Li XP, Li G, Peng Y, Kung HF, Lin MC. Suppression of Epstein–Barr virus-encoded latent membrane protein-1 by RNA interference inhibits the metastatic potential of nasopharyngeal carcinoma cells. Biochem Biophys Res Commun 2004;315:212–8.
[22] Hu LF, Zabarovsky ER, Chen F, Cao SL, Ernberg I, Klein G, et al. Isolation and sequencing of the Epstein–Barr virus BNLF-1 gene (LMP1) from a Chinese nasopharyngeal carcinoma. J Gen Virol 1991;72:2399–409 (Pt 10).
[23] Chen ML, Tsai CN, Liang CL, Shu CH, Huang CR, Sulitzeanu D, et al. Cloning and characterization of the latent membrane protein (LMP) of a specific Epstein–Barr virus variant derived from the nasopharyngeal carcinoma in the Taiwanese population. Oncogene 1992;7:2131–40.
[24] Li SN, Chang YS, Liu ST. Effect of a 10-amino acid deletion on the oncogenic activity of latent membrane protein 1 of Epstein–Barr virus. Oncogene 1996;12:2129–35.
[25] Tsai CN, Tsai CL, Tse KP, Chang HY, Chang YS. The Epstein–Barr virus oncogene product, latent membrane protein 1, induces the downregulation of E-cadherin gene expression via activation of DNA methyltransferases. Proc Natl Acad Sci USA 2002;99:10084–9.
[26] Lu J, Chua HH, Chen SY, Chen JY, Tsai CH. Regulation of matrix metalloproteinase-1 by Epstein–Barr virus proteins. Cancer Res 2003;63:256–62.
[27] Wang LT, Lin CS, Chai CY, Liu KY, Chen JY, Hsu SH. Functional interaction of Ugene and EBV infection mediates tumorigenic effects. Oncogene 2011;30:2921–32.
[28] Li X, Liu X, Li CY, Ding Y, Chau D, Li G, et al. Recombinant adeno-associated virus mediated RNA interference inhibits metastasis of nasopharyngeal cancer cells in vivo and in vitro by suppression of Epstein–Barr virus encoded LMP-1. Int J Oncol 2006;29:595–603.
[29] Tang KF, Tan SY, Chan SH, Chong SM, Loh KS, Tan LK, et al. A distinct expression of CC chemokines by macrophages in nasopharyngeal carcinoma: implication for the intense tumor infiltration by T lymphocytes and macrophages. Hum Pathol 2001;32:42–9.
[30] Chow KP, Wu CC, Chang HY, Chang C, Chang YS. A simplified tumour model established via Epstein–Barr virus-encoded, nasopharyngeal carcinoma-derived oncogene latent membrane protein 1 in immunocompetent mice. Lab Anim 2008;42:193–203.
[31] Sriadibhatla S, Yang Z, Gebhart C, Alakhov VY, Kabanov A. Transcriptional activation of gene expression by pluronic block copolymers in stably and transiently transfected cells. Mol Ther 2006;13:804–13.
[32] Hung TH, Li YH, Tseng CP, Lan YW, Hsu SC, Chen YH, et al. Knockdown of c-MET induced apoptosis in ABCB1-overexpressed multidrug-resistance cancer cell lines. Cancer Gene Ther 2015;22:262–70.
[33] Sathy BN, Chou YH, Li HJ, Chang C, Chow KP. Dynamic contrast-enhanced and T2-weighted magnetic resonance imaging study of the correlation between tumour angiogenesis and growth kinetics. Lab Anim 2009;43:53–9.
[34] Jahr S, Hentze H, Englisch S, Hardt D, Fackelmayer FO, Hesch RD, et al. DNA fragments in the blood plasma of cancer patients: quantitations and evidence for their origin from apoptotic and necrotic cells. Cancer Res 2001;61:1659–65.
[35] Pantel K, Alix-Panabieres C, Riethdorf S. Cancer micrometastases. Nat Rev Clin Oncol 2009;6:339–51.
[36] Cvitkovic E, Bachouchi M, Boussen H, Busson P, Rousselet G, Mahjoubi R, et al. Leukemoid reaction, bone marrow invasion, fever of unknown origin, and metastatic pattern in the natural history of advanced undifferentiated carcinoma of nasopharyngeal type: a review of 255 consecutive cases. J Clin Oncol 1993;11:2434–42.
[37] King AD, Ahuja AT, Leung SF, Lam WW, Teo P, Chan YL, et al. Neck node metastases from nasopharyngeal carcinoma: MR imaging of patterns of disease. Head Neck 2000;22:275–81.
[38] Husemann Y, Geigl JB, Schubert F, Musiani P, Meyer M, Burghart E, et al. Systemic spread is an early step in breast cancer. Cancer Cell 2008;13:58–68.
[39] Rocken M. Early tumor dissemination, but late metastasis: insights into tumor dormancy. J Clin Invest 2010;120:1800–3.
[40] Eyles J, Puaux AL, Wang X, Toh B, Prakash C, Hong M, et al. Tumor cells disseminate early, but immunosurveillance limits metastatic outgrowth, in a mouse model of melanoma. J Clin Invest 2010;120:2030–9.
[41] McAllister SS, Weinberg RA. The tumour-induced systemic environment as a critical regulator of cancer progression and metastasis. Nat Cell Biol 2014;16:717–27.
[42] Olechnowicz SW, Edwards CM. Contributions of the host microenvironment to cancer-induced bone disease. Cancer Res 2014;74:1625–31.
[43] Hellevik T, Martinez-Zubiaurre I. Radiotherapy and the tumor stroma: the importance of dose and fractionation. Front Oncol 2014;4:1.
[44] Yoon SK. Recent advances in tumor markers of human hepatocellular carcinoma. Intervirology 2008;51(Suppl. 1):34–41.
[45] Zetter BR. Angiogenesis and tumor metastasis. Annu Rev Med 1998;49:407–24.